Supplemental Figure 1

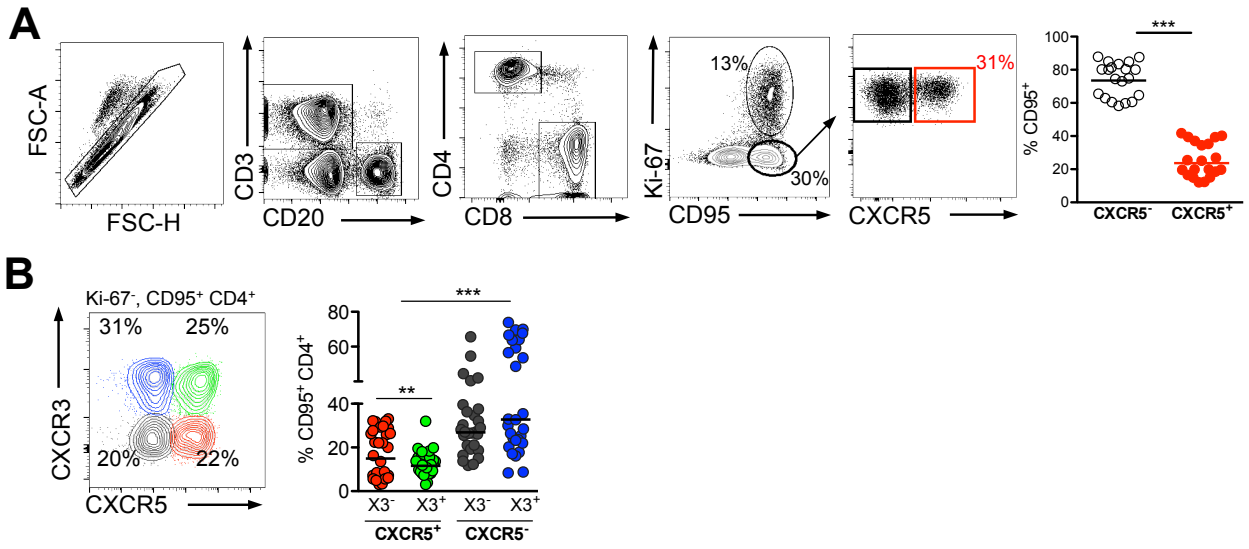

Supplemental Figure 1: Distribution of CXCR5 subsets on memory CD4 T cells (A) Gating strategy to examine $CD4^+$ T cells and distribution of CXCR5 on quiescent memory CD4 T cells (B) Distribution of X5 and X3 subsets among non-cycling memory cells and frequencies shown in scatter plot.

Supplemental Figure 2

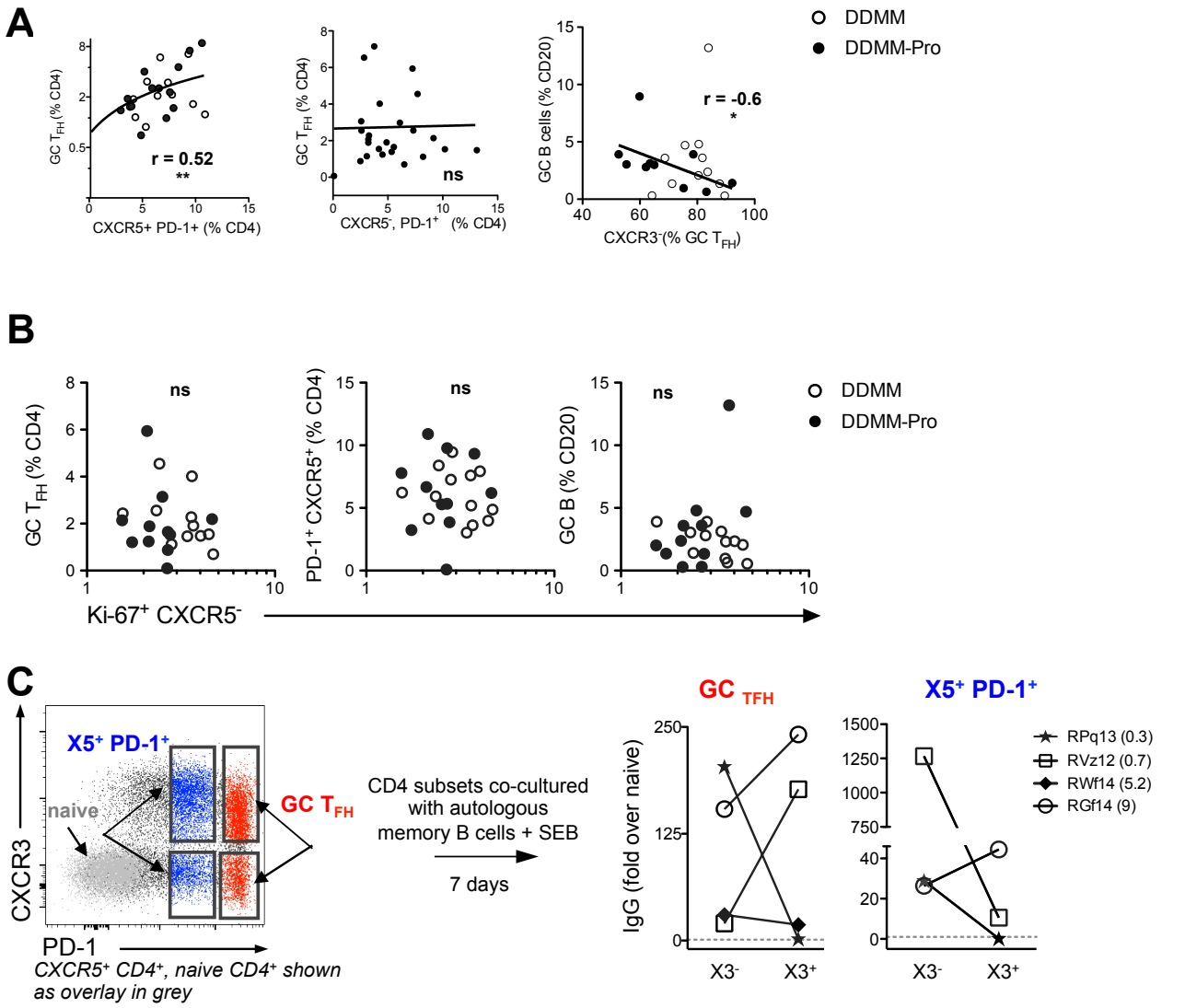

Supplemental Figure 2: Association between lymph node CXCR5$^+$ and CXCR5$^-$ subsets. GC T_{FH} cells positively correlate with (A) CXCR5$^+$ PD1$^+$ cells but do not associate with CXCR5$^-$, PD-1$^+$ CD4$^+$ T cells. Right panel in A shows inverse association between CXCR3$^-$ GC T_{FH} cells and GC B cell frequencies. (B) Ki-67$^+$ CXCR5$^-$ CD4 T cells at peak post 2nd MVA do not correlate with GC T_{FH} cells, CXCR5$^+$ PD-1$^+$ cells, and with GC B cells. (C) Indicated CD4 subsets from lymph node at 2 weeks post 2nd MVA were FACS sorted and co-cultured with autologous memory B cells in the presence of SEB. IgG in supernatant is expressed in X3$^-$ and X3$^+$ GC T_{FH} and CXCR5$^+$ PD1$^+$ subsets as fold increase over IgG in naive-B cell co-cultures. Data are shown for 4 animals assayed independently and values in parenthesis indicate IgG in supernatant (pg/mL) in naive-B cell co-cultures.

Supplemental Figure 3

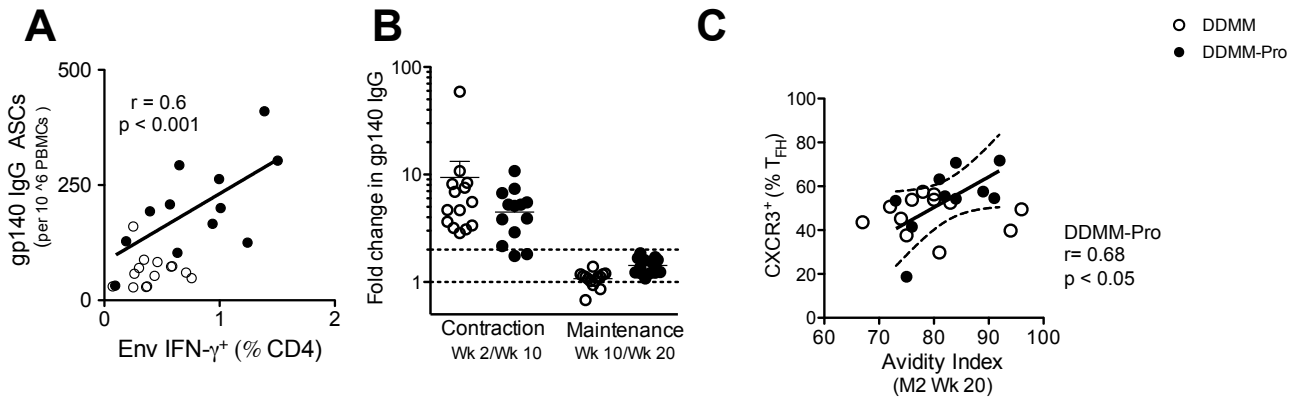

Supplemental Figure 3: Determinants of vaccine-induced B cell responses. (A) Gp140 ASC response correlate with Env IFNγ^+ CD4 responses (B) Antibody titers undergo contraction between week 2 to week 10 after 2nd MVA boost and are largely maintained from week 10 to week 20 (C) CXCR3 expression on T_{FH} cells directly correlates with antibody avidity.

Supplemental Figure 4

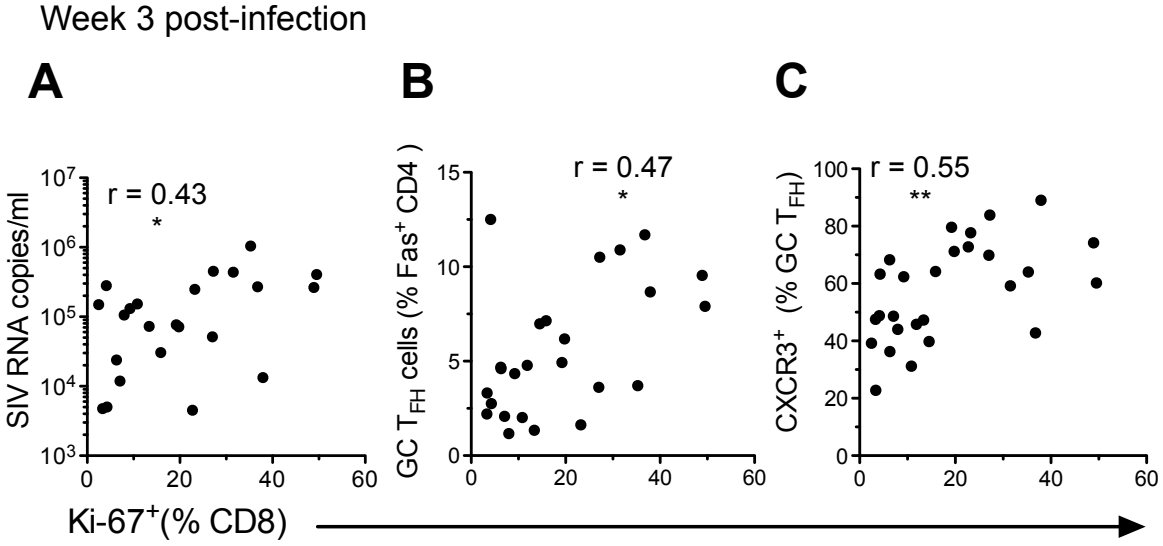

Supplemental Figure 4: Association between Ki-67$^+$ CD8 T cell responses and GC T_{FH} cell responses at 3 weeks post-infection. Frequency of Ki-67$^+$ CD8 T cells in blood correlate with concurrent measurements of (A) peak plasma viral load (B) GC T_{FH} cells (C) CXCR3$^+$ GC T_{FH} cells.